BRUKER TechNote #201

A Comprehensive Guide to Photothermal AFM-IR Spectroscopy

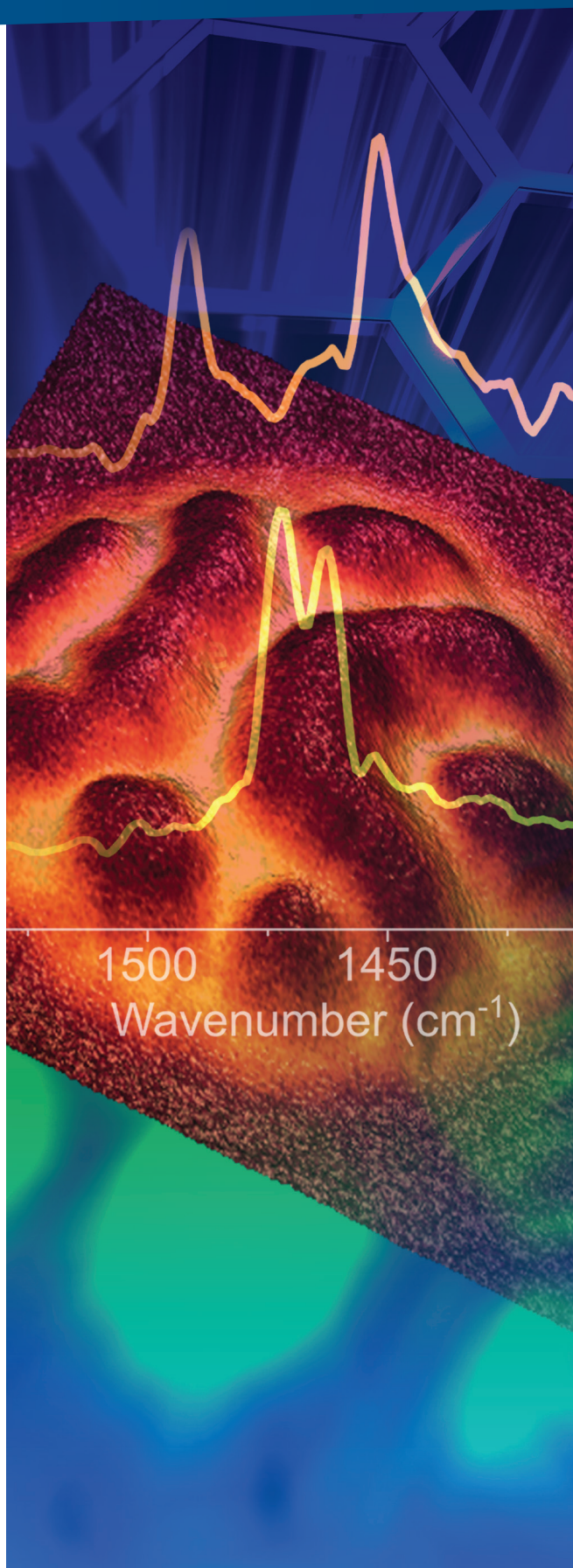

Photothermal atomic force microscope infrared spectroscopy (AFM-IR) enables chemical identification at the nanoscale by collecting local infrared spectra at the AFM tip, which correlate with bulk Fourier transform infrared (FTIR) spectra. Compared to other nanoscale spectroscopic techniques, such as scattering scanning nearfield optical microscopy (s-SNOM) and tip-enhanced Raman spectroscopy (TERS), AFM-IR provides major advantages in ease of use, ease of interpretation, measurement speed, and data repeatability. A typical AFM-IR spectrum takes only several seconds, resulting in fast collection of point spectra and reasonable collection times for hyperspectral imaging. The AFM-IR technique can also achieve monolayer sensitivity, sub-10 nm spatial resolution, and a range of probing depths. However, a number of experimental factors may impact IR band intensities, positions, and shapes, and thus need to be considered to interpret AFM-IR spectra. This technical note describes the capabilities of photothermal AFM-IR and the experimental factors that can impact spectral interpretation.

Introduction to Photothermal AFM-IR

Photothermal AFM-IR, often referred to as simply AFM-IR, is an analytical technique used for chemical identification at nanoscale levels. AFM-IR combines the nanoscale spatial resolution of atomic force microscopy with the chemical analysis capability of infrared spectroscopy. Individually, atomic force microscopy is routinely used for high-resolution imaging of diverse samples to obtain topographic, mechanical, electrical, and other properties. Using a sharp tip, it achieves a spatial resolution of <10 nm and in some cases can resolve down to the molecular or even atomic scale. Infrared spectroscopy is a powerful optical technique that enables chemical identification, since each material has its own characteristic absorption bands in the "fingerprint" region due to its specific molecular vibrations. By combining these two techniques together, AFM-IR can achieve chemical identification with a spatial resolution several orders of magnitude below the optical diffraction limit, which typically has a value of several to multiple tens of microns for a mid-infrared source.

Compared to other complementary nanoscale infrared spectroscopy techniques—most notably scattering scanning near field optical microscopy (s-SNOM) and tip-enhanced Raman spectroscopy (TERS)—AFM-IR is easier to operate, and the AFM-IR spectra have better correlation with FTIR spectra. AFM-IR measures the cantilever oscillation signal, which is directly proportional to the infrared absorption by the sample. In comparison, the established technique

to measure the complex optical properties of samples, s-SNOM, uses more complicated interferometric detection and relies on theoretical modeling. This often results in spectra suffering from peak shifts, as well as band shapes and peak ratios inconsistent with the FTIR spectrum.[1] Raman spectroscopy is another powerful and widely adopted analytical technique for molecular identification and structural analysis. The Raman scattering process has a very low cross section, especially for vibrations involving light elements, and relies heavily on the manufacturing of field-enhancing tips for TERS, leading to limited consistency and limited reproducibility. TERS acquired from protein molecules often lack amide bands, which limits their utilization for a determination of protein secondary structure.[2] AFM-IR stands out from s-SNOM and TERS in its close correlation with transmission FTIR spectra in terms of peak shapes, positions, band ratios, and high signal-to-noise ratios.

Infrared Spectroscopy Reference Chart

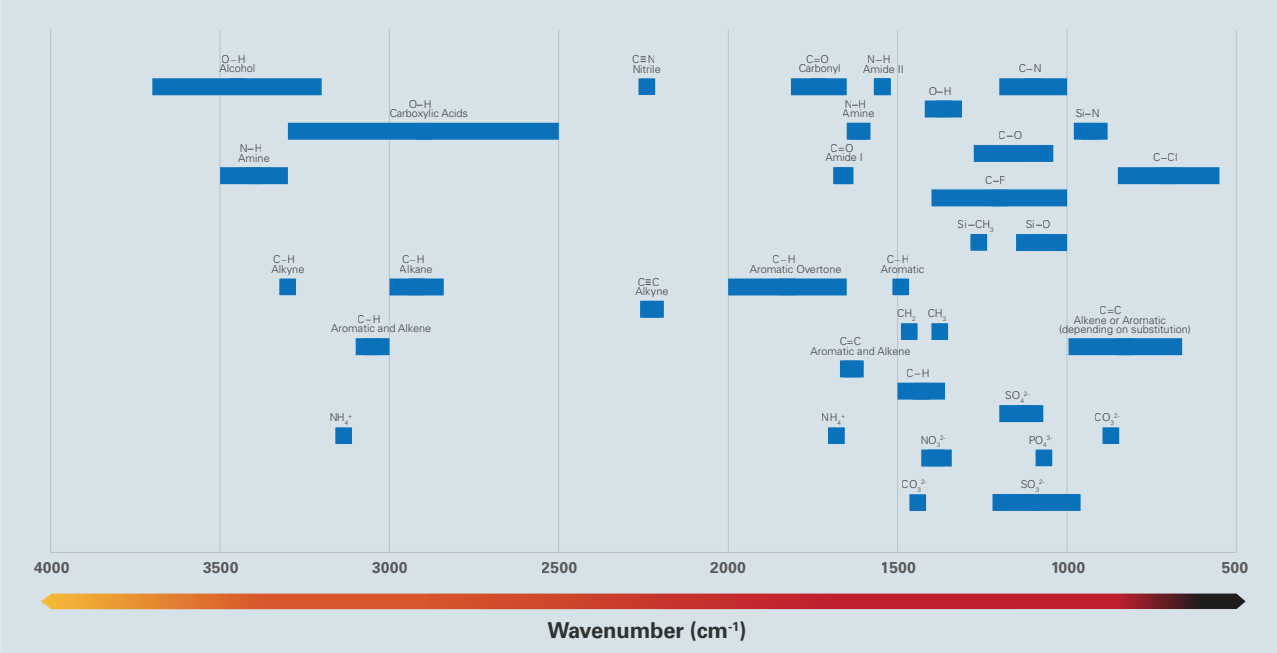

FIGURE 1. Typical IR absorption frequencies for common functional groups. (See full-page printable chart on page 19).

The AFM-IR technique was first developed by Alexandre Dazzi using a "bottom up" configuration,[3] and commercial instrumentation based on this technique (nanoIR™) was first developed in 2010 by Anasys Instruments, which was acquired by Bruker in 2018. Over the years, technological improvements have dramatically advanced AFM-IR capabilities in terms of sensitivity, spatial and spectral resolutions, measurement time, and fields of applications. Later generations of nanoIR instruments (nanoIR2™, nanoIR3™) adopted a "top down" configuration, which does not require an IR-transparent substrate and greatly improves the variety of samples that can be studied. The Dimension IconIR™ system is based on Bruker's industry-leading Dimension Icon® AFM platform and is currently the most advanced, highest-performance AFM-IR instrument in the world due to the low noise and high stability of its AFM, high sensitivity and multiple modes of AFM-IR measurement, and available correlative studies of mechanical, electrical, and thermal properties.

Working Principles

AFM-IR works by using an AFM tip to locally detect a sample's thermal expansion resulting from absorption of infrared radiation at the tip location. In this way, a spatial resolution on the scale of the AFM tip radius is achieved. In AFM-IR measurements, a pulsed infrared laser beam is focused onto a region of a sample in the proximity of the AFM tip. Absorption of the infrared beam causes an instantaneous thermal expansion of the sample, which induces a transient force on the AFM cantilever that drives the cantilever into oscillation. The cantilever oscillation could be over a mixture of multiple oscillatory eigenmodes in conventional AFM-IR mode, or a certain eigenmode could be selectively enhanced in Resonance-Enhanced or Tapping AFM-IR modes.

AFM-IR spectra are obtained by measuring the AFM cantilever oscillation amplitude as a function of wavelength while maintaining the AFM tip at stationary xy positions on the sample. AFM-IR maps that show the distribution of chemical species across a sample are created by scanning the sample while illuminating it with fixed wavelengths. With the improvement of measurement speed, hyperspectral imaging (in which full AFM-IR spectra are measured on a dense grid of points) has become more popular, and it provides richer information about molecular species and their distributions in the sample.

Experimentally, AFM-IR requires a pulsed laser source together with optics for beam steering, focusing, and polarization control. To maintain the laser alignment to the tip, a sample xy scanner is required. With a small temperature rise (<10 K with OPOs; <1 K with QCLs) and a typical thermal expansion coefficient (10^{-6} to 10^{-4}), the resulting photothermal expansion is on the scale of several to tens of picometers for a polymer sample with a thickness of hundreds of nanometers. The rapid sample thermal expansion changes the instantaneous equilibrium position of the cantilever, converting the thermal expansion on the scale of tens of picometers into cantilever oscillations on the nanometer scale. With the improvement of sensitivity, the AFM-IR technique is now capable of detecting a single monolayer sample with a thermal expansion orders of magnitude lower.

The physics of how AFM-IR works is straightforward and well-understood. The overall AFM-IR signal intensity due to the infrared absorption by the sample at the tip location is expressed as:[4,5]

$$S_{\text{AFM-IR}} \propto H_{\text{AFM}} H_{\text{exp}} I_{\text{inc}}(\lambda)\, \alpha(\lambda)$$

EQUATION 1.

where H_{AFM} and H_{exp} are contributions from the AFM cantilever oscillation dynamics and the sample thermal expansion coefficient, $I_{inc}(\lambda)$ is the laser power at the tip, and $\alpha(\lambda) = 4\pi\kappa(\lambda)/\lambda$ is the sample absorption coefficient at the wavelength λ with $\kappa(\lambda)$ as the imaginary part of sample refractive index.

From the above equation, while the AFM-IR signal intensity does depend on other material properties of the sample, such as thermal expansion coefficient and mechanical stiffness, these properties remain constant at a specific point on the sample, so they do not affect the relative peak intensities or peak shapes. Therefore, the AFM-IR signal measured as the oscillation amplitude of the cantilever at a fixed point (X_0, Y_0) on a sample is directly proportional to the absorption coefficient:

$$S_{\text{AFM-IR}}(X_0, Y_0) \propto \alpha(\lambda, X_0, Y_0)$$

EQUATION 2.

and the AFM-IR spectrum directly correlates to the bulk FTIR spectra collected in transmission mode. This lays the foundation for the use of AFM-IR as a nanoscale chemical identification technique, as the AFM-IR spectra can be digitally searched against commercial databases of FTIR spectra and otherwise identified like any typical transmission FTIR spectrum.

AFM-IR spectra have been shown to correlate to transmission FTIR spectra for a wide range of materials. Below is the comparison of an AFM-IR spectrum collected from a polystyrene film of 300 nm thickness to an FTIR transmission spectrum. The spectra show very good correlation in both the CH-stretching region (2800-3200 cm^{-1}) and the fingerprint region (1000-1800 cm^{-1}).[6,7] This highlights the strength of AFM-IR spectroscopy as a chemical identification technique at nanometer spatial scales, something not achievable using conventional FTIR instrumentation.

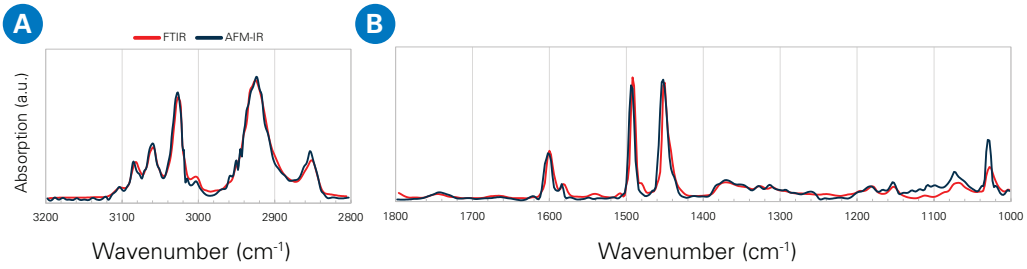

FIGURE 2. Comparison of AFM-IR and bulk FTIR spectra of a polystyrene film: (a) CH-stretching region, (b) fingerprint region.

Major Operational Modes

Since the invention of the AFM-IR technique, several different AFM-IR modes have been developed by Bruker and collaborators, including Resonance-Enhanced, Tapping AFM-IR, PeakForce IR, and Surface Sensitive modes.

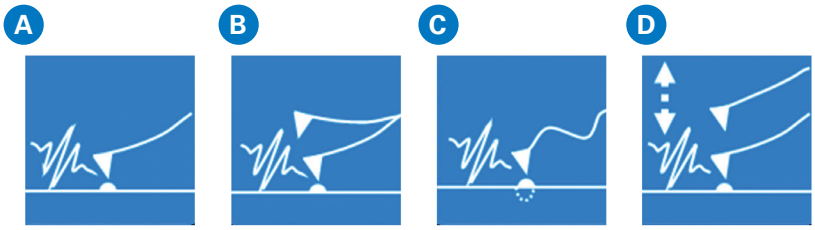

FIGURE 3. Major AFM-IR modes: (a) contact or Resonance-Enhanced mode, (b) Tapping AFM-IR mode, (c) Surface Sensitive mode, and (d) PeakForce Tapping AFM-IR mode.

Each mode has demonstrated unique strengths and has significantly extended AFM-IR capabilities, enabling major breakthroughs in numerous research fields. When choosing a mode for AFM-IR measurement, it is important to consider the sample properties and the goal of the measurement. A summary of the AFM-IR modes, the laser source used, sensitivity, spatial resolution, and likely applications are presented in Table 1.

TABLE 1. Major AFM-IR modes implemented on the nanoIR/IconIR systems

Mode	Laser source	Sensitivity	Spatial resolution (nm)	Applications
Conventional	Ekspla OPO	>50 nm	>50	Polymeric and biological material with thickness >50 nm
Resonance-Enhanced	Daylight QCL, M Squared Firefly; APE Carmina	monolayer	>20	Monolayer, single molecule
Tapping AFM-IR	Daylight QCL, M Squared Firefly; APE Carmina	monolayer	<10	Loose particle, soft/sticky material
Surface Sensitive	Daylight QCL,M Squared Firefly; APE Carmina	monolayer	<10	Multilayer, thin coating on bulk

Conventional AFM-IR Mode

AFM-IR has traditionally been operated in contact mode, with simple signal acquisition and low demands on the light source while still providing the key advantage of correlation to transmission FTIR. The ringdown of the AFM cantilever oscillations after the sample absorbs radiation is analyzed via the fast Fourier transform (FFT) technique to extract their amplitudes and frequencies. By measuring the peak-to-peak intensity of the cantilever ringdown or the amplitude of the cantilever oscillation at a selected frequency as a function of the source wavelength, local absorption spectra can be created.

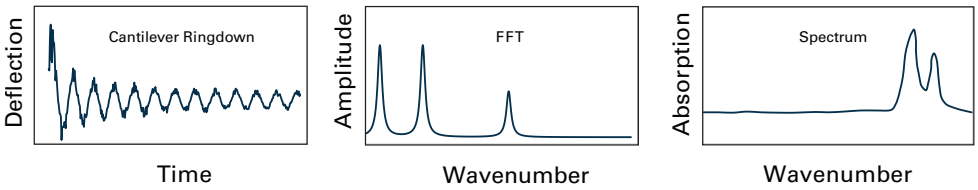

FIGURE 4.
Diagrams of the cantilever ringdown, FFT, and spectrum for conventional AFM-IR operation.

The conventional AFM-IR mode typically requires a sample thickness of more than 50 nm to obtain a detectable AFM-IR signal. An AFM-IR spectrum with a range of 1000 cm^{-1} takes approximately 2-4 minutes to obtain, as the laser wavelength is tuned slowly in a step-by-step manner.

Resonance-Enhanced AFM-IR Mode

The development of Bruker's patented Resonance-Enhanced mode was an important breakthrough resulting in significant improvements in the sensitivity of AFM-IR that leverages advances in Quantum Cascade Laser (QCL) technology.[8] The mid-infrared laser source used is usually a QCL or an M Squared Firefly laser, both with a tunable pulse repetition rate. The AFM cantilever is engaged with the sample in contact mode, and the laser pulse repetition rate is tuned to match a contact resonance frequency of the cantilever. Absorption of infrared radiation by the sample causes thermal expansion, which results in continuous excitation of the cantilever. This is different than conventional AFM-IR, which shows decay in the ringdown. Any contact resonance frequency can be selected for AFM-IR measurements. For AFM-IR spectroscopy, the second cantilever resonance frequency near 180 kHz is typically selected, as it has a good signal-to-noise ratio. A Resonance-Enhanced AFM-IR spectrum is obtained by plotting the amplitude of a selected cantilever resonance in the frequency domain as a function of the laser wavelength. For AFM-IR imaging, a higher resonance frequency (>1 MHz) may be selected, as it provides higher spatial resolution due to the shorter thermal diffusion length between two adjacent laser pulses.

The Resonance-Enhanced mode significantly improves AFM-IR sensitivity due to the enhancement of the AFM cantilever oscillation. The AFM-IR signal boost or gain from resonant excitation is $Q/(2\pi)$, where Q is the quality factor of the cantilever mode, defined as the resonance amplitude over its full width at half maximum. The typical signal amplification is 5 to 40 times with respect to the ringdown mode. This allows for AFM-IR measurements on thin samples, such as a self-assembled monolayer with thickness as low as <1 nm on a silicon substrate. The high sensitivity of this mode has enabled measurements of infrared absorption spectra and chemical maps for a single protein molecule, with the results facilitating the accurate determination of the secondary structure of a single protein molecule that is consistent with the structure of the bulk protein material.[9] Compared to the conventional AFM-IR mode, the spatial resolution of Resonance-Enhanced mode is improved and can extend down to 20 nm for relatively smooth samples. The speed of Resonance-Enhanced AFM-IR spectroscopy is also improved, as the laser wavelength is usually scanned in a fast sweep mode. A spectrum with a range of 1000 cm^{-1} is typically obtained in just 1–10 seconds.

To compensate for the mechanical difference between different components of the sample, a phase-locked loop (PLL) is usually implemented to maintain the match between the laser pulse rate and the contact resonance frequency of the cantilever on the sample.

Tapping AFM-IR Mode

The implementation of AFM-IR measurements utilizing a tapping technique represents another important advancement. Bruker's invention of TappingMode™ enabled high-resolution topography measurements on rough, soft, or adhesive samples, which were previously

challenging or impossible in contact mode. The same is true for Tapping AFM-IR.[10,11] Tapping AFM-IR improves spatial resolution significantly, to below 10 nm, and even less than 5 nm in some measurements. This improvement in spatial resolution makes it possible to obtain meaningful infrared absorption images on samples with fine structures, such as block copolymers and some semiconductor samples with small domains. Like Resonance-Enhanced mode, Tapping AFM-IR has achieved high sensitivity to measure thin monolayer samples.

Tapping AFM-IR employs a heterodyne detection scheme, where the laser pulse repetition rate is tuned to match the sum or difference of the two lowest resonance frequencies (f_1 and f_2) of the cantilever. The AFM cantilever operates in TappingMode, in which the probe is driven by a piezo actuator with periodic oscillations at one of the cantilever resonance frequencies (f_2 or f_1) so that the tip intermittently contacts (i.e., "taps") the sample. The Tapping AFM-IR signal is detected at another resonance frequency (f_1 or f_2) and is proportional to the absorption coefficient of the sample at the tip location.[10]

A QCL or Firefly laser is typically used for the Tapping AFM-IR mode. Two different Tapping AFM-IR probes are used: The semi-soft TnIR-A probe operates with a driving frequency near 60 kHz at the first mode and a detection frequency near 380 kHz at the second mode. The more rigid TnIR-D probe operates with a driving frequency near 1600 kHz at the second mode and is detected at the first mode near 250 kHz. Currently, TnIR-D probe is used as the default probe for Tapping AFM-IR due to its higher signal-to-noise ratio.

Surface Sensitive AFM-IR Mode

Surface Sensitive AFM-IR mode (SSM) is a newly developed Bruker proprietary mode aimed at measuring only the top layer of a sample by limiting signal contributions from sub-surface material.[12] It has the potential to measure the top layer of a sample without much preparation, and its full capabilities are still being explored.

In SSM, a soft AFM cantilever is engaged with the sample in contact mode. Heterodyne detection is used where the laser pulse repetition rate is tuned to match the sum or difference of two contact resonance frequencies of the cantilever. This mode is different from Tapping AFM-IR, which uses two tapping frequencies. In SSM, the cantilever is driven at a high resonance frequency near 2 MHz and detected at a lower resonance frequency such as ~180 kHz, with a relatively high laser pulse repetition rate. This combination of experimental settings provides higher surface sensitivity than Resonance-Enhanced mode or even Tapping AFM-IR mode. For a typical polymer sample, SSM is capable of limiting signal contributions to only the top 10–30 nm of the sample.

PeakForce Tapping AFM-IR Mode

Bruker and our research customers frequently develop innovative new modes. The PeakForce Tapping AFM-IR (PFIR) mode has been developed by Bruker collaborator Xiaoji Xu and co-workers, as an emerging powerful mode of the AFM-IR technique.[13] PFIR leverages Bruker's patented PeakForce Tapping® mode, in which the AFM tip intermittently contacts the sample by performing approach and retraction routines at several kilohertz. Smart synchronized averaging and background subtraction mechanisms enable PeakForce Tapping to operate at far higher speeds than conventional force curves, while retaining the advantages of the off-resonant approach, i.e., delivering quantitative nanomechanical data. PFIR leverages the contact time during each PeakForce Tapping cycle to transduce the infrared absorption of the sample, delivering infrared spectroscopy and imaging capability at sub-10 nm spatial resolution.

By precisely controlling the interaction force between the AFM probe and the sample, PFIR is particularly useful on rough and sticky samples. Since PFIR utilizes PeakForce Tapping, one major benefit is the capability to simultaneously map several important material properties, including topographic, chemical, mechanical (e.g., adhesion, modulus), and electrical (e.g., surface potential).

AFM-IR in Liquid Mode

IR spectroscopic measurements of samples in liquid are of interest and importance, as some samples (such as biological species) exist in a native liquid environment and drying them could result in structural changes or loss of certain functionalities. Conventionally, such measurements have been thought impossible due to strong absorption of mid-infrared by water. Despite this challenge, an AFM-IR in Liquid mode has been developed on the nanoIR system using bottom-up illumination. The AFM-IR in Liquid mode has allowed researchers to resolve the secondary structures of protein samples in water, and results showed that AFM-IR spectra and maps of samples in water have comparable signal-to-noise ratio and lateral resolution as in air.[14] Further work showed that Tapping AFM-IR works better than Resonance-Enhanced mode for samples in a fluid environment. These developments generate new possibilities for AFM-IR analysis of a wide range of samples that are air-sensitive.

As alternatives to immersion in a liquid phase, some samples could also be prepared as nano droplets on a substrate using nano spray, or sealed in a hydrated environment with a thin hydrogel coating.[15,16] These new techniques allow samples to be measured using the standard top-down illumination and are much more likely to preserve the native structures in liquid.

Experimental Accessories

Laser Sources

The availability of wavelength-tunable lasers is a critical enabling factor for AFM-IR experiments. There have been a variety of light sources adopted for AFM-IR measurements over the years, and each has its own strengths and limitations. The choice of light source for an AFM-IR experiment depends on the specific requirements of the measurement, such as the desired spectral range, spectral resolution, output power, pulse repetition rate of the laser, and the size and cost constraints of the AFM system being used.

So far, all of the lasers used for AFM-IR spectroscopy emit linearly polarized light. In addition to the tip enhancement, light polarization can be leveraged to determine the molecular orientation and structure of the sample and to efficiently excite or launch optical modes. In recent years, there have been many advances in light sources for AFM-IR, and the development of new sources continues to expand the capabilities of AFM-IR for a wide range of applications.

TABLE 2. Laser sources commonly used on the nanoIR/IconIR systems.

Laser	Coverage (cm^{-1})	Pulse repetition rate (kHz)	Spectral resolution (cm^{-1})	Scan speed (cm^{-1}/s)	Measurement time
Daylight QCL	750–3000 (3–4 chips for 1000 cm^{-1} range)	0.1–3000	<1	Typical 100 for spectroscopy	1–10 s
M Squared Firefly	~2700–4000	130–300	4–8	~100	10–20 s
APE Carmina	670–2200 for AFM-IR	50–1500	10–15	20–40	~1 min
Ekspla OPO	~1000–3600	1	4–8	4	Several mins

QCLs are currently the most commonly used lasers for AFM-IR measurements. The QCLs from Daylight Solutions have pulse repetition rates tunable over a wide range, from below 1 kHz to a maximum of 3 MHz, making them compatible with all major AFM-IR modes including Resonance-Enhanced, Tapping AFM-IR and Surface Sensitive modes. Daylight QCL offers a wide range of coverage from 750–3000 cm^{-1}, with a spectral resolution of <1 cm^{-1}. A single QCL chip typically covers a range of about 300 cm^{-1}, so the fingerprint region of 800–1800 cm^{-1} requires three or four chips to cover this entire range. Up to four QCL chips can be housed in the same laser module. For regular AFM-IR spectroscopic measurements, the QCL laser is typically swept at a speed of around 100 cm^{-1}/s, which provides a balance between good signal to noise and data acquisition time. For hyperspectral imaging, a much higher sweep speed of around 1000 cm^{-1}/s is typically used. This allows for high-speed data acquisition and enables the acquisition of a large number of spectra in a short period of time.

The latest QCL laser from Daylight Solutions has the "zero-pointing" option, which maintains a stable laser beam pointing over the entire tuning range. This feature reduces the need for correction to bring the laser beam to the AFM tip location, improving the accuracy and reproducibility of AFM-IR measurements.

The Firefly laser from M Squared has a coverage of 2700–4000 cm^{-1}, which is useful for studying the stretching modes of C-H, N-H, and O-H. Most Firefly lasers on the nanoIR or IconIR systems have a pulse repetition rate of 130–300 kHz, which is suitable for Resonance-Enhanced AFM-IR with a cantilever contact resonance frequency of around 180 kHz. To use the Firefly laser at higher frequency (>300 kHz) for Resonance-Enhanced mode or Tapping AFM-IR mode, a harmonic ($n \geq 2$) is applied. For example, if a theoretical pulse repetition rate of 1 MHz is desired, the Firefly laser can be set at 250 kHz with a harmonic number n=4, or at 200 kHz with a harmonic number n=5. The Firefly laser has a spectral resolution of 4–8 cm^{-1}. AFM-IR spectral measurement is performed by sweeping the laser at a constant speed, which typically takes 10–20 seconds to complete a scan of the entire range.

The Carmina laser developed by APE GmbH is primarily used on the nanoIR3-s broadband system, as it enables spectroscopic measurements for both AFM-IR and s-SNOM. For AFM-IR, the laser is tunable in the range of 670–2200 cm^{-1} with a spectral resolution of 10–15 cm^{-1}. The laser has a pulse repetition rate of 50–1500 kHz, making it compatible with Resonance-Enhanced, Tapping AFM-IR, and Surface Sensitive AFM-IR measurements.

Historically, OPO lasers from Ekspla Inc. were used for earlier nanoIR systems. Most of these lasers cover a wide mid-IR range, from around 1000–4000 cm^{-1}. OPO lasers in the near IR or visible range (wavelengths 400–2600 nm) have also been used. The laser has a fixed pulse repetition rate of 1 kHz, and a spectral resolution of 4–8 cm^{-1}. It is tuned in a slow step mode for spectroscopic measurements, which can take several minutes for one individual spectrum.

There are other narrowband or broadband sources that can be used for nanoIR systems. Narrowband laser sources, such as a single-line CO_2 laser, can be modulated with an acoustic optical modulator (AOM) or a mechanical chopper. Broadband sources, such as synchrotron or supercontinuum lasers, when integrated with a beam modulator and an FTIR unit, can also be used for AFM-IR measurements. All these light sources provide researchers with a range of additional options, each with its own unique capabilities, to choose from when performing AFM-IR measurements. Our application experts can advise on selection of the best-suited source solution for your applications.

Typical AFM Probes

TABLE 3. AFM probes commonly used for AFM-IR measurements.

Probe	Nom. Length (µm)	Nom. Tip Radius (nm)	Nom. Spring Constant (N/m)	Gold Coating Thickness (nm)	AFM-IR Mode	Nom. Resonance Frequency (kHz)
CnIR-B	450	20	0.2	70	Resonance-Enhanced, SSM	~180 (2nd mode) for RE, >1000 (drive), 180 (detect) for SSM
TnIR-A	225	<25	3	70	Resonance-Enhanced, Tapping	~300 for RE, 60 (drive), 380 (detect) for Tapping
TnIR-D	125	20	40	50	Tapping	1600 (drive), 250 (detect)

The AFM probe is a crucial element to obtain quality AFM-IR data. For earlier nanoIR systems with a bottom-up illumination, no infrared beam shines directly on the cantilever, which allows for little restriction on the probe selection, enabling the use of common silicon or silicon nitride probes. As the technique has become more advanced, Bruker has developed a family of probes optimized for different AFM-IR applications. To have the best AFM-IR signal, metal-coated (usually gold) probes in certain geometries are used. By reflecting most of the incoming illumination, the metal coating helps to minimize absorption of the infrared beam by the cantilever arm. This results in purer AFM-IR signal from the sample. The metal coating also helps to enhance the AFM-IR signal by increasing the electric field of the infrared illumination near the sharp AFM tip.

The CnIR-B probe is selected for both Resonance-Enhanced and Surface Sensitive modes. It is a soft probe with a cantilever length of 450 µm and a spring constant of 0.2 N/m, which provides a good balance between sensitivity and stability. In Resonance-Enhanced mode, the probe is driven at one of the contact resonance frequencies. For spectroscopic measurement in this mode, the signal is typically detected at the second resonance near 180 kHz, providing a high signal-to-noise ratio. For Surface Sensitive mode, the probe is typically driven at a higher resonance above 1 MHz and detected at the resonance near 180 kHz.

The TnIR-A probe is selected for use in both Resonance-Enhanced and Tapping AFM-IR modes. The semi-rigid probe has a cantilever length of 225 µm and a spring constant of 3 N/m. In Resonance-Enhanced mode, the probe operates at the contact resonance frequency near 300 kHz, and the AFM-IR signal is recorded at this frequency. In Tapping AFM-IR, the probe is driven at the first resonance frequency of 60 kHz and detected at the second resonance frequency of 380 kHz.

The TnIR-D probe is selected specifically for Tapping AFM-IR mode. It is a rigid probe with a cantilever length of 125 µm and a high spring constant of 40 N/m. In Tapping AFM-IR mode, the probe is typically driven at the second resonance near 1.6 MHz and detected at the first resonance near 250 kHz. The high sensitivity and high spatial resolution of AFM-IR measurements that can be achieved with the TnIR-D probe make it an attractive option for a wide range of applications.

Understanding Photothermal AFM-IR Spectroscopy

The correlation between AFM-IR spectra and far-field bulk FTIR spectra is well understood and has been demonstrated over the past ten years through numerous publications. This correlation establishes AFM-IR as a reliable and powerful nanoscale chemical identification technique, and has driven the adoption of AFM-IR within the analytical chemistry community and beyond. Despite this correlation, various experimental factors could affect the relative intensities of IR absorption bands and peak ratios in the AFM-IR spectra. To correctly analyze and interpret AFM-IR data, it is critical to have a good understanding of these impacting factors.

Impact of the IR Laser

Variations Caused by the Laser Beam

Several laser beam-based factors could impact the measured AFM-IR spectra, including attenuation, pointing, and collimation.

Attenuation

As shown earlier in Equation 1, the AFM-IR signal is proportional to the laser power $I_{inc}(\lambda)$ and the sample absorption coefficient $\alpha(\lambda)$, thus normalization of the signal by the laser power would give the absorption spectrum that directly correlates to the FTIR spectrum in transmission mode. Thus for each AFM-IR experiment, a laser background file is recorded first by measuring the laser power as a function of wavelength using a power meter. Then, the AFM-IR signal is normalized by the laser power at each step in the spectral range. This method has been validated in a large number of application examples, but can be insufficient in some cases.

During AFM-IR measurements, the laser power is typically attenuated using a set of mesh filters. The attenuation percentage of the mesh filters is calibrated at a fixed wavenumber (for example, 1600 cm^{-1}) but actually changes as a function of wavelength. The deviation from the calibrated attenuation percentage becomes more pronounced at lower laser power (<5%), thus impacting peak ratios of the AFM-IR spectrum, since the signal is usually normalized to unattenuated laser power (100%). There are two compensation options to account for this deviation:

1. The laser background can be recorded at the same percentage as in the AFM-IR spectrum; however, this background will have a lower signal-to-noise ratio than the laser power curve collected at 100%.

2. One or multiple polarizers can be used to attenuate the laser power. Though this corrects the attenuation fluctuation, it could introduce beam distortion due to the nonideal parallelism of the polarizers.

Pointing and Collimation

Variations in the laser beam pointing and collimation can cause fluctuations in the AFM-IR signal and affect peak ratios of the infrared absorption bands. Variations in beam pointing can be corrected by a set of two fast steering mirrors in the beam path. The mirror positions are calibrated for several selected wavelengths, then extrapolated for other wavelengths in the spectral range. The latest model of QCL laser from Daylight includes a "zero-pointing" option that reduces fluctuations in beam pointing from wavelength to wavelength, improving the accuracy of the AFM-IR signal. Variations in beam collimation can be corrected by automatically adjusting the focusing distance of an off-axis parabolic (OAP) mirror to the AFM tip, so that maximum signal is obtained for each wavelength in the spectral range.

QCL Chip Transition

For a spectral range of 800–1800 cm^{-1} covered by four QCL chips, each of the three chip transitions could lead to artifacts in the AFM-IR spectrum. The artifacts may show up as jumps or dips in the spectrum at wavenumbers corresponding to the chip transitions. They are usually caused by sudden changes in beam pointing, focusing, or laser output power across the chip transitions. The latest "zero-pointing" model can help alleviate the impact of chip transitions, and is included standard in Bruker systems. When picking QCL chips, it is recommended to avoid chip transitions in the middle of important absorption bands. For example, in biological studies, it is desirable not to have chip transitions within the amide I or II bands, around 1660 and 1540 cm^{-1} respectively. Finally, artifacts in the spectra due to chip transitions are well understood and can be analyzed and corrected in post processing in the nanoIR/IconIR software using mathematical methods.

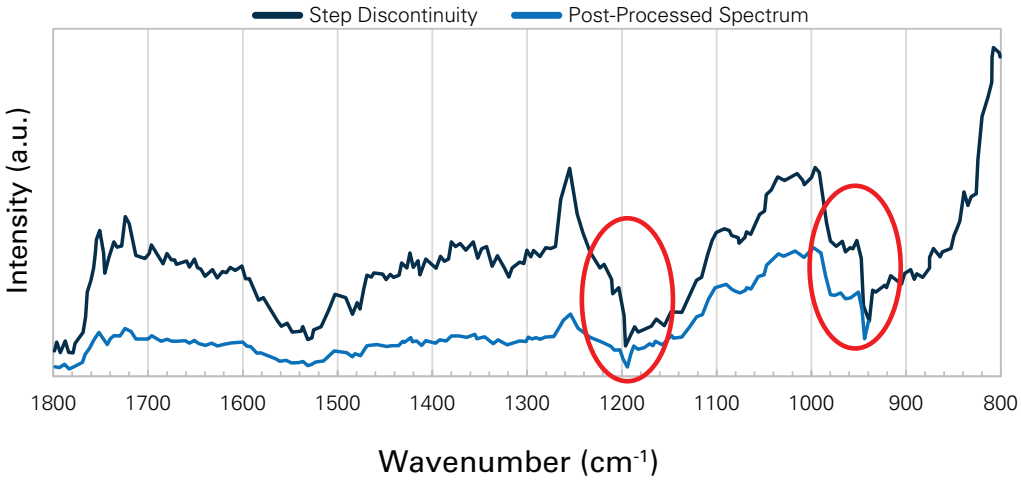

FIGURE 5.
Comparison of AFM-IR spectra before and after correction of QCL chip transitions.

Impact of the AFM Probe

AFM Cantilever Arm Absorption (SiO, SiN)

In nanoIR/IconIR systems with top-down illumination, metal-coated (mostly gold) AFM probes are used. The gold coating usually has a thickness of >50 nm and covers the whole cantilever arm, to minimize the background. In this way, AFM-IR signal purely from the sample is measured. In case the coating is too thin or does not cover enough, part of the infrared beam may penetrate through the coating and get absorbed by the SiN/SiO material of the cantilever arm. This will cause the AFM cantilever to oscillate and contribute to the overall signal, resulting in a broad absorption feature or elevated baseline near 1000–1200 cm^{-1} in the AFM-IR spectrum. Probes from new batches are pre-tested by Bruker to minimize this risk.

AFM Tip Contamination (PDMS)

AFM-IR is a high sensitivity technique that can detect a monolayer or even single protein molecule in the sample. Such high sensitivity also applies when there is even a tiny amount of contaminant on the AFM tip. Infrared absorption bands due to contaminants, predominantly polydimethylsiloxane (PDMS), have been observed in Tapping AFM-IR spectra collected with Tapping AFM-IR probes. As shown in the FTIR spectrum in Figure 6, the PDMS has broad absorption features of Si-O-Si stretch at 1020 and 1090 cm^{-1}, and a sharper band assigned to $Si-CH_3$ umbrella mode at 1260 cm^{-1}. Bruker's current technology has greatly reduced PDMS contamination, and new processes have been introduced to qualify probes during each step in manufacturing, storage, and shipping.

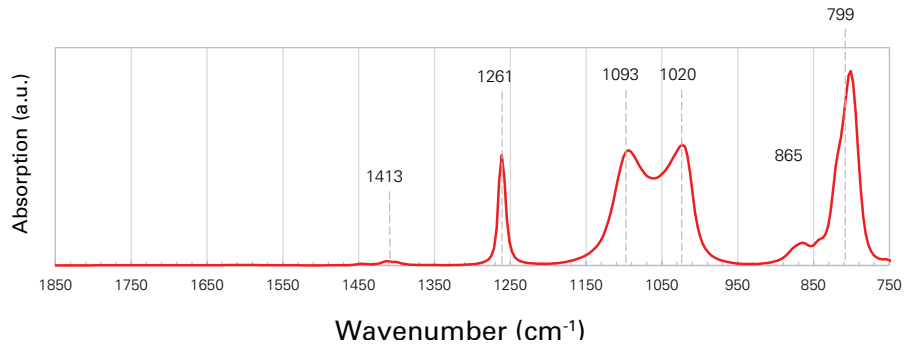

FIGURE 6.
FTIR spectrum of PDMS.

Shift of Resonance Frequency and PLL

Phase lock-in loop (PLL) has been implemented in Resonance-Enhanced, Tapping AFM-IR, and Surface Sensitive modes. PLL enables tracking of the cantilever resonance frequencies, and adjusting of the laser repetition rate accordingly to match the resonance frequency (for Resonance Enhanced mode) or sum/difference of two resonance frequencies (for Tapping AFM-IR and Surface Sensitive modes). The cantilever resonance frequencies could shift as a result of AFM tip interactions with a heterogeneous sample, as shown in Figure 7. Such a shift during AFM-IR measurements can reduce the signal intensity and change the relative intensities of IR absorption bands in the AFM-IR spectrum. In AFM-IR images of samples with multiple components that have different mechanical stiffness, shifts in the cantilever resonance frequencies due to mechanical difference could give rise to extra contrast or even the appearance of some high-resolution features at the boundary of different components. To minimize the impact of cantilever resonance shift, it is recommended to enable the PLL whenever possible during AFM-IR measurements, with the acquired frequency providing complimentary information on the sample mechanical stiffness.

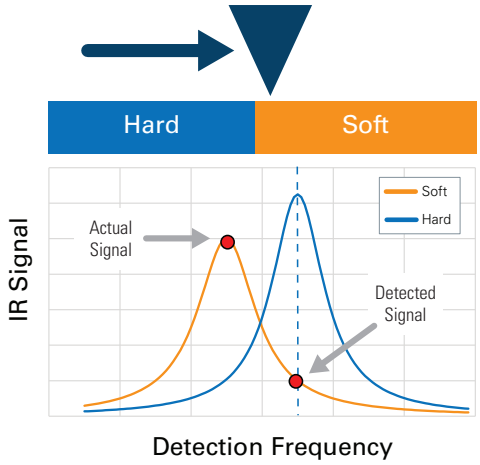

FIGURE 7.
Shift of resonance frequency with material stiffness.

Impact of Sample and Substrate

Sample Softening or Melting

In standard operation during AFM-IR measurements, the sample temperature rises a few degrees or less, which induces a tip oscillation signal. In extreme cases, absorption of laser irradiation can lead to sample softening or melting if the laser power is too high, which may irreversibly damage the sample. This usually happens at wavelengths where laser power is high and/or the sample has strong absorption, such as the polymethylmethacrylate (PMMA) carbonyl stretching band at 1730 cm^{-1}. Sample softening or melting may be indicated by a sudden shift of the cantilever resonance frequency, and in some cases may be verified by a bump or dip at the measurement location in the AFM topography image collected afterwards. With softening or melting, the sample thermal expansion is significantly greater than normal, which leads to artificially strong signals in the AFM-IR spectrum.

Sample softening and melting can be easily avoided by starting at low laser powers (for example, 2%), then increasing gradually to ensure that the sample temperature does not rise excessively. The cantilever resonance frequency can then be monitored during the AFM-IR measurements to look for any drift that may indicate softening.

Sample Thickness

AFM-IR can accommodate samples with a wide range of thicknesses. As discussed previously, different AFM-IR modes provide different options for probing depth, typically a few hundred nanometers to several microns for Resonance-Enhanced mode, 50–100 nm for Tapping AFM-IR, and 10–30 nm for Surface Sensitive mode.

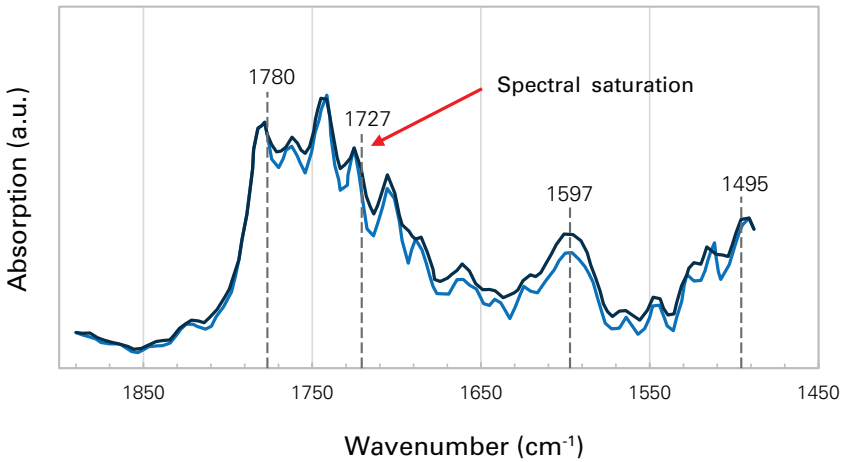

FIGURE 8.
AFM-IR spectrum of a thick polymer film sample showing spectral saturation.

Most samples measured by AFM-IR have a thickness ranging from a monolayer (several nanometers or less) to several micrometers. For samples with large thickness, signal saturation can become an issue, similar to that observed in transmission mode FTIR. Infrared wavelengths with stronger absorption are attenuated faster as it propagates into the sample, while infrared wavelengths with weaker absorption can propagate further. This effect would result in flattened tops of strong absorption bands and increased intensities of weaker absorption bands in the AFM-IR spectrum, as shown in Figure 8. On the other hand, if the sample is thinner than the probing depth of the AFM-IR mode used, absorption of the infrared beam by material underneath the substrate will contribute to the overall signal. In Figure 9, Resonance-Enhanced and Surface Sensitive AFM-IR spectra of a thin coating on a bulk material are compared. The differences show that Surface Sensitive mode is detecting only the thin coating, while Resonance-Enhanced mode collected a mixed signal from both coating and bulk. Therefore, it is important to select the proper AFM-IR mode for measurements and to consider the impacts of these factors when interpreting the AFM-IR spectrum.

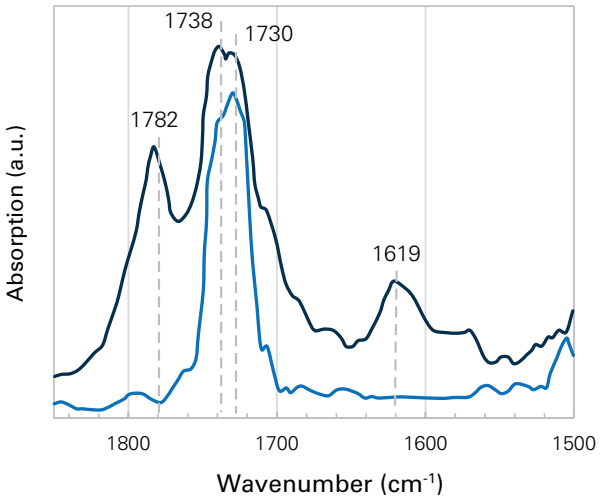

FIGURE 9.
AFM-IR spectra collected with Resonance-Enhanced mode (dark blue) and Surface Sensitive mode (light blue) of a sample with 50 nm thin coating on a 1 µm thick film sample.

Molecular Orientation and Laser Polarization

The nanoIR/IconIR systems are capable of probing molecular orientation, as lasers integrated in the systems have a linear polarization, which is usually oriented normal to the sample surface (vertical, or p-polarized). For samples with preferred molecular orientations, the vertical polarization of the laser beam will generate a relatively stronger AFM-IR signal for molecular vibrations with electric dipole-transition moments oriented perpendicular to the sample plane rather than in the sample plane. This follows the same selection rule as in FTIR and results in different peak ratios in the AFM-IR spectrum for samples with preferred molecular orientation compared to those with random molecular orientation.

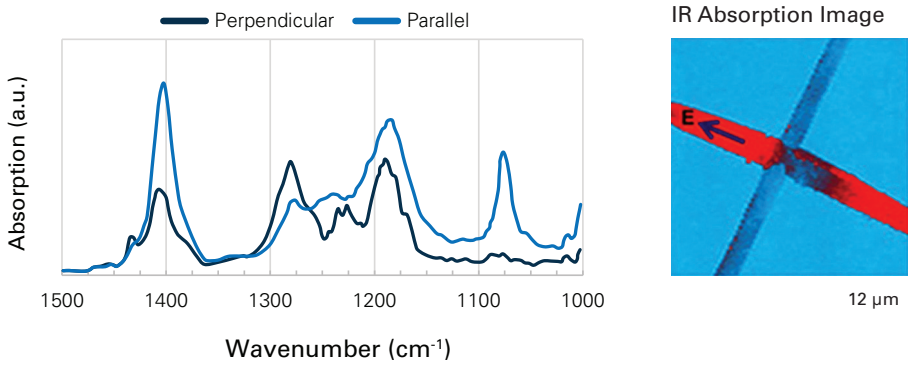

FIGURE 10.
(left) AFM-IR spectra of PVDF fiber with infrared polarization parallel to and perpendicular to the fiber orientation; (right) infrared absorption image at 1404 cm^{-1} with IR polarization along one of the two fibers.

Furthermore, the gold-coated AFM tip enhances the electric field of the laser radiation, especially when the laser polarization is parallel to the AFM tip. However, the enhancement factor may not be constant across the spectral range. As a result, it could enhance the intensities of some infrared bands more than others, changing peak ratios in the AFM-IR spectrum.

Photoacoustic Effect

Absorption of the infrared beam by samples in the illumination area could generate a photoacoustic wave that interacts with the cantilever arm and creates probe excitation in addition to signal from the AFM tip location. In AFM-IR measurements, the focused IR spot has a typical diameter of about 50 µm. If there is absorbing material within this area near the cantilever arm, artifacts from the photoacoustic wave could be observed in the AFM-IR spectra or images.[17,18] To minimize the photoacoustic effect, it is recommended to avoid having large amounts of absorbing material right under the cantilever arm. Preparing samples with diluted absorbing material could reduce the effect. For an existing sample, the orientation of the sample relative to the AFM tip could be adjusted so that there is less absorbing material under the cantilever arm.

Substrate Effects

The substrate plays a critical role in multiple ways, including signal enhancement. For samples with weak signals, a metal substrate (typically gold) can be used to enhance the electric field of the laser irradiation and generate a stronger AFM-IR signal. This has been demonstrated in measurements on thin films, monolayers, single protein molecules, etc. Metal substrates are still widely used to enhance signal, even though the AFM-IR technique has reached the sensitivity of detecting a single layer of molecules on non-metal substrates.

The substrate can also contribute to the overall signal by absorbing the infrared beam. For example, a silicon substrate typically has a thin layer of SiO_2 on top that absorbs near 1100 cm^{-1} and then releases heat to the softer sample above. As a result, some AFM-IR signal may be observed near 1100 cm^{-1}, even if the sample itself does not absorb in that spectral range.

One more factor to consider is substrate reflectance, which varies as a function of wavelength.[19] After the laser beam penetrates the sample and reaches the substrate, certain wavelengths are reflected more than others. This reflected beam has a second chance of getting absorbed by the sample, leading to a stronger AFM-IR signal.

Applications of AFM-IR Spectroscopy

AFM-IR spectroscopy has well-understood physics that offer direct correlation to bulk transmission FTIR. This theoretical correlation has now been realized in practice thanks to engineering efforts to minimize AFM-IR artifacts, giving AFM-IR legitimacy as a reliable chemical identification technique. AFM-IR has an ever-increasing number of applications in such fields as polymer science, biology, optics, geology, pharmaceutics, drug delivery, optoelectronics, chemistry, corrosion science, 2D materials, art conservation, and others. In this section, a few interesting application examples are presented to highlight the correlation between AFM-IR spectroscopy and bulk FTIR.

Quantitative Analysis of PE/PP Polymer Blends

AFM-IR spectroscopy has the capability to quantify the concentration of polymeric components in nanoscale domains of complex polymer blends. Though much of the work using AFM-IR is qualitative, Su et al. used AFM-IR to quantitatively study polymeric component distribution in high impact polypropylene (HIPP) by way of a calibration curve.[20] HIPP has two components, polyethylene (PE) and polypropylene (PP), and can form three phases: matrix, intermediate layer, and core (Figure 11a and b). As a first step, the AFM-IR spectra of pure PE and PP were collected and confirmed to match the FTIR spectra in the spectral range of interest in terms of peak position and relative intensity. While PE shows only the symmetric bending band of the methylene (CH_2) group at 1456 cm^{-1}, PP has an additional symmetric bending band of the methyl (CH_3) group at 1378 cm^{-1} (Figure 11c). By changing the weight percentages of PE/PP, a calibration curve of the 1456/1378 cm^{-1} peak ratio as a function of the weight percentage was built (Figure 11d). The calibration showed excellent linear correlation and satisfactory agreement between AFM-IR and FTIR.

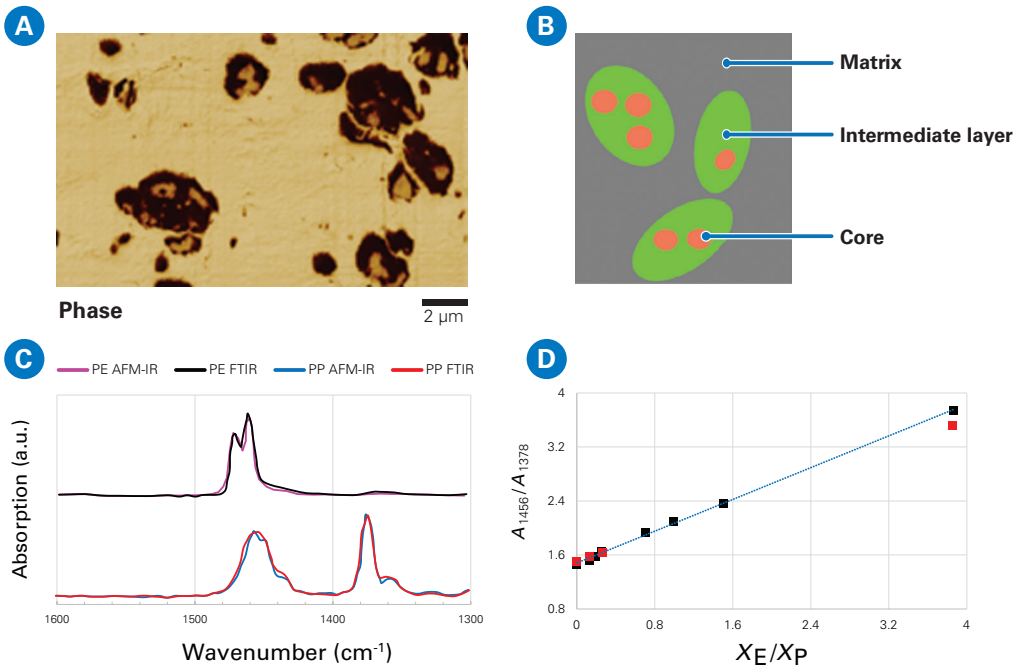

FIGURE 11. Quantitative analysis of PE/PP blends. Adapted with permission from F Tang, P Bao, and Z Su, Analytical Chemistry 88, 4926 (2016). DOI: 10.1021/acs.analchem.6b00798. Copyright 2016 American Chemical Society.

Based on the calibration curve, AFM-IR spectra were collected from the three phases of HIPP, and then analyzed to quantify the percentages of the PE/PP components in each phase. It was found that the PE content in the matrix was close to zero and was high in the rubbery intermediate layers, and PP was the major component of the rigid cores.

Single Protein Molecule

The high sensitivity of the AFM-IR technique has been demonstrated in a number of applications, and is best shown in the measurements of the AFM-IR spectrum and absorption image for a single protein molecule.[9] To achieve such high sensitivity, Ruggeri et al. used an off-resonance, low power, and short pulse of the infrared beam to excite the single protein molecule. Such an experimental scheme gave the maximum contrast in laser-induced cantilever deflection signal between the protein sample and the gold substrate, while avoiding damage of the soft protein sample during the measurement (Figure 12a).

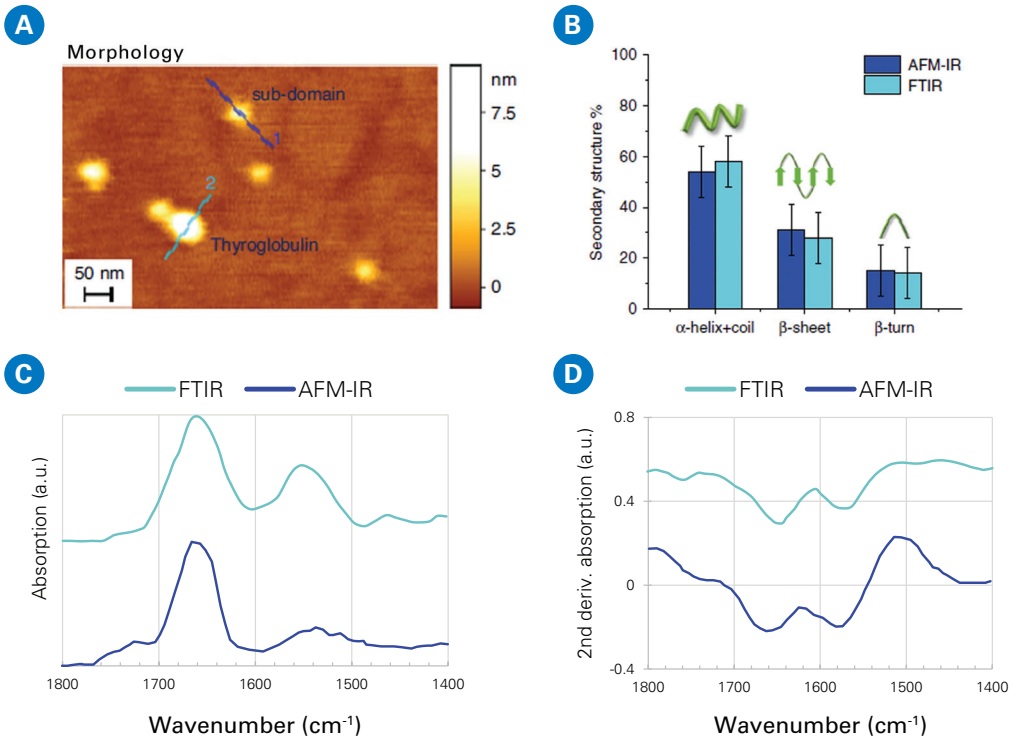

FIGURE 12.
AFM-IR spectrum of a single protein molecule. Adapted from F S Ruggeri, B Mannini, R Schmid, M Vendruscolo, and T P J Knowles, Nature Communications 11, 2945 (2020). DOI: 10.1038/s41467-020-16728-1, licensed under CC BY 4.0.

AFM-IR spectra were collected from a single molecule of the thyroglobulin protein. The individual spectrum was acquired on a time scale of 1 second, with a signal-to-noise ratio of 10–20. The AFM-IR spectrum clearly showed amide I and II bands, which resemble the infrared bands in the FTIR spectrum recorded for bulk thyroglobulin protein (Figure 12c). The high signal-to-noise ratio and detailed shape of the amide I band allowed determination of the protein secondary structure. To do that, the AFM-IR spectrum was performed with second derivative analysis and compared to the FTIR (Figure 12d). Results from the AFM-IR measurement showed three major components of the secondary structure, α-helix + coil, β-sheet, and β-turn, with the percentage of each secondary structure being consistent with that measured by FTIR spectrum for bulk thyroglobulin protein material (Figure 12b).

Low-*k* Dielectrics in a Semiconductor

Low-k dielectric materials is a keen area of research for the semiconductor industry due to their capability to reduce capacitive signal delays. Previously, infrared spectroscopic studies of low-k dielectrics have been limited to examining blanket films or micron-wide ordered arrays of patterned structures. AFM-IR has enabled the characterization of low-k dielectrics at nanoscale dimensions.

In one study, a low-*k* sample of a-SiOC:H/Cu with a periodic interconnect structure at the nanoscale was measured with AFM-IR.[21] Although the low-*k* a-SiOC:H dielectric has a relatively low coefficient of thermal expansion, characteristic infrared absorption bands were clearly observed in the AFM-IR spectra. In the 2800–3200 cm^{-1} range that encompasses the symmetric and asymmetric C-H stretching modes, strong correlation was observed between the AFM-IR and FTIR spectra (Figure 13a). In the lower wavenumber range, the two spectra also showed good correlation for Si-O-Si "cage" mode (1150 cm^{-1}), the symmetric $Si(C\text{-}H_3)_x$ deformation mode (1275 cm^{-1}), the $Si\text{-}CH_2\text{-}Si$ wagging mode (1360 cm^{-1}), and the asymmetric $Si(C\text{-}H_3)_x$ deformation mode (1410 cm^{-1}). The AFM-IR spectrum showed a weaker infrared band by the Si-O-Si network mode (1050 cm^{-1}), which was attributed to the different incidence angles of infrared beams with linear polarizations in the AFM-IR from FTIR. Nevertheless, the general correlation between AFM-IR and FTIR spectra is quite convincing.

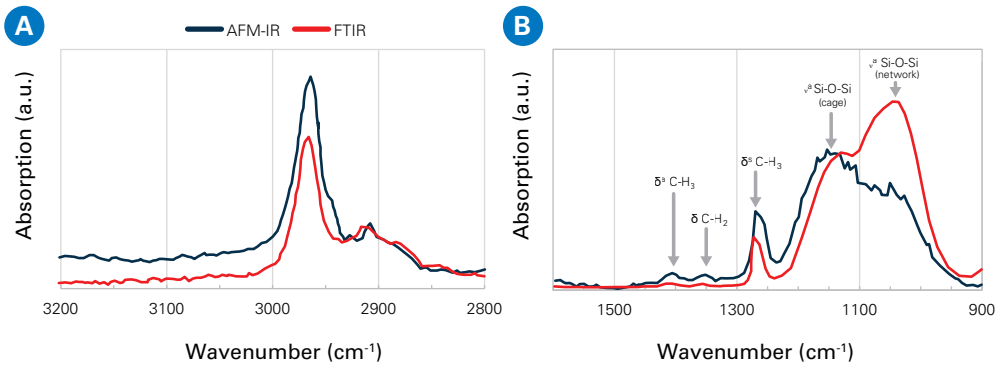

FIGURE 13.
AFM-IR spectrum of low-*k* dielectrics. Adapted from Ref. 21 with permission. Copyright 2015 The Electrochemical Society.

Aerosol Particles

Nanoscale aerosol particles are abundant in the air and can act as cloud condensation nuclei. To understand the physical properties and chemical reactivities of the aerosol particles, and thus their impacts in the atmosphere, it is critical to identify their morphologies and chemical compositions. Grassian et al. have used AFM-IR to investigate single and multi-component systems comprised of inorganic salts and organic compounds relevant to the atmosphere.[22]

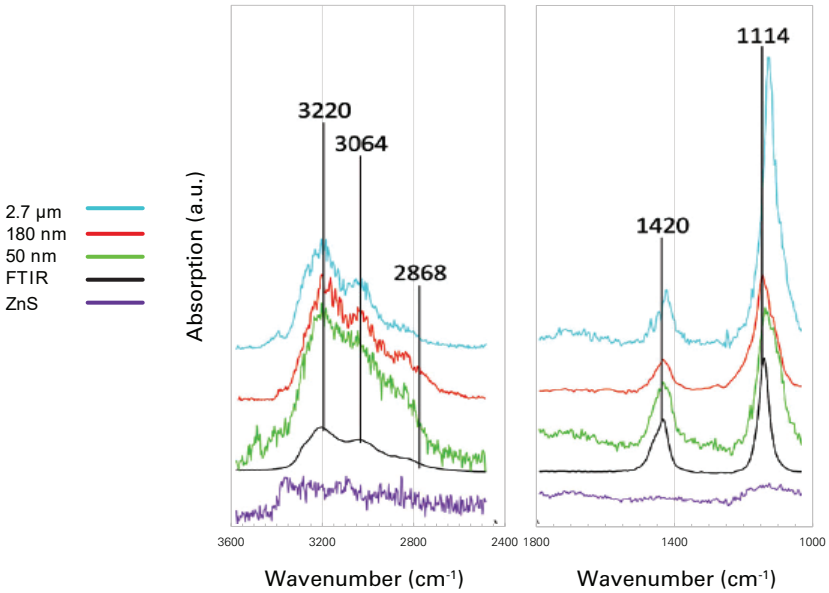

FIGURE 14.
AFM-IR spectrum of an individual ammonium sulfate aerosol particle. Adapted from Ref. 22 with permission. Copyright 2018 The Royal Society of Chemistry.

In one study, several model aerosol particles were prepared and then measured on a single-particle basis. For the ammonium sulfate particles, AFM-IR spectra were collected in the ranges of 2400–3600 cm^{-1} and 1000–1800 cm^{-1} from particles with a diameter of 2.7 µm, 180 nm, and 50 nm (Figure 14). Overall, the AFM-IR spectra showed comparable infrared bands due to the vibrational modes of $\nu_3(NH_4^+)$ (3230, 3064, 2868 cm^{-1}), $\nu_4(NH_4^+)$ (1424 cm^{-1}), and $\nu_3(SO_4^{2-})$ (1120 cm^{-1}). Absorption bands in the AFM-IR spectrum from an ammonium sulfate particle with a small diameter of 50 nm are clearly distinguishable.

Silk Protein Fiber

Silk protein fibers are renowned for their unparalleled mechanical strength and extensibility arising from their high β-sheet crystalline contents as natural materials. This protein species can go through conformational transitions induced by electron beam lithography. Tao et al. have demonstrated the capability to control and characterize the structure of individual silk protein fibers using a combination of the electron beam lithography and AFM-IR techniques.[23]

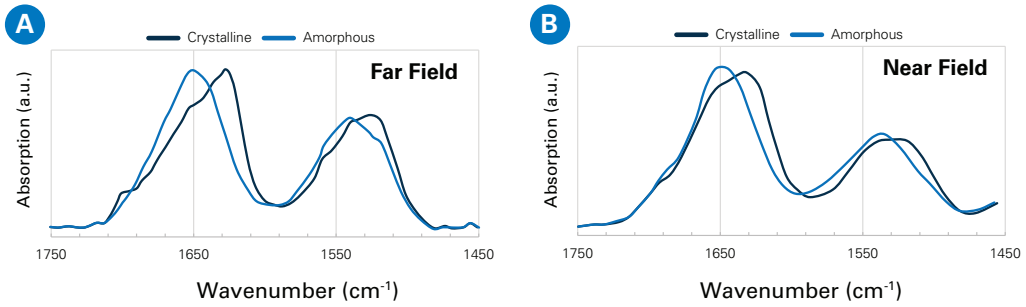

FIGURE 15.
(a) FTIR and (b) AFM-IR spectra of crystalline and amorphous silk protein. Adapted from N Qin et al., Nature Communications 7, 13079 (2016). DOI: 10.1038/ncomms13079, licensed under CC BY 4.0.

An AFM-IR spectrum recorded over the amide I and II regions showed that the crystalline form has a higher content of β-sheet conformation at 1625 cm^{-1}. With conformational change induced by the electron beam, the β-sheet content decreased while the amorphous content at 1645 cm^{-1} increased. The AFM-IR spectrum showed the same trend as the bulk FTIR spectrum, as shown in Figure 15. The results demonstrated that the AFM-IR spectrum correlates well with the FTIR spectrum, while providing the capability to measure an individual silk protein fiber in a heterogeneous sample without averaging signal collected from a bulk amount of material.

Conclusions

Photothermal AFM-IR is a technique that has well-understood physics and correlates well with transmission FTIR data, enabling key insights from bulk spectroscopy to be applied directly at the nanoscale. Due to working at the nanoscale, several factors need to be considered in the measurement, processing, and characterization of AFM-IR spectra, which have been addressed in this technical note. By understanding these key factors, AFM-IR spectroscopy allows for sub-diffraction measurements that can be used on polymer, biological, semiconductor, and inorganic samples to offer rich new characterization pathways to materials researchers.

www.bruker.com/nanoIR

Infrared Spectroscopy Reference Chart

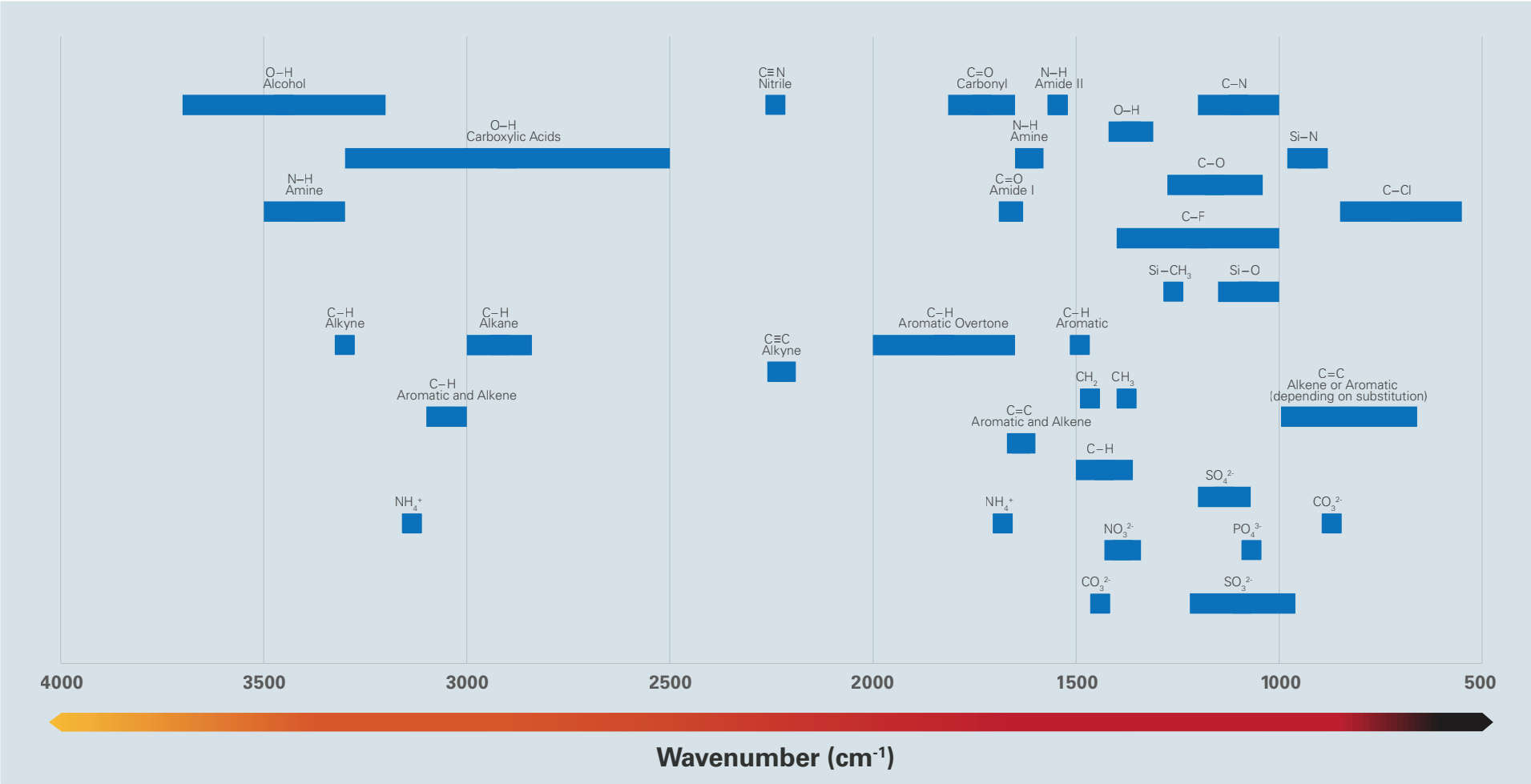

References

1. A C Jones, and M B Raschke, *Nano Letters* 12, 1475 (2012). DOI: 10.1021/nl204201g
2. D Kurouski, *Vibrational Spectroscopy 91*, 3 (2017). DOI: 10.1016/j.vibspec.2016.06.004
3. A Dazzi, R Prazeres, F Glotin, and J M Ortega, *OPTICS LETTERS 30*, 2388 (2005). DOI: 10.1364/ol.30.002388
4. A Dazzi, F Glotin, and R Carminati, Journal of *Applied Physics 107*, 124519 (2010). DOI: 10.1063/1.3429214
5. J J Schwartz, D S Jakob, and A Centrone, *Chemical Society Reviews 51*, 5248 (2022). DOI: 10.1039/D2CS00095D
6. C Marcott, M Lo, K Kjoller, C Prater, and I Noda, *Applied Spectroscopy 65*, 1145 (2011). DOI: 10.1366/11-06341
7. A Dazzi, and C B Prater, *Chemical Reviews 117*, 5146 (2017). DOI: 10.1021/acs.chemrev.6b00448
8. F Lu, M Jin, and M A Belkin, *Nature Photonics 8*, 307 (2014). DOI: 10.1038/nphoton.2013.373
9. F S Ruggeri, B Mannini, R Schmid, M Vendruscolo, and T P J Knowles, *Nature Communications 11*, 2945 (2020). DOI: 10.1038/s41467-020-16728-1
10. J Mathurin, E Pancani, A Deniset-Besseau, K Kjoller, C B Prater, R Gref, and A Dazzi, *Analyst 143*, 5940 (2018). DOI: 10.1039/C8AN01239C
11. F Tarpoudi Baheri, T M Schutzius, D Poulikakos, and L D Poulikakos, *Journal of Microscopy 00*, 1 (2020). DOI: 10.1111/jmi.12890
12. International Patent WO2020049053; United States Patent US 11,215,637 B2
13. L Wang, H Wang, M Wagner, Y Yan, D S Jakob, X G Xu, *Science Advance 3*, e1700255 (2017). DOI: 10.1126/sciadv.1700255
14. G Ramer, F S Ruggeri, A Levin, T P J Knowles, and A Centrone, *ACS Nano 12*, 6612 (2018). DOI: 10.1021/acsnano.8b01425
15. A Miller, S Chia, Z Toprakcioglu, T Hakala, R Schmid, Y Feng, T Kartanas, A Kamada, M Vendruscolo, F S Ruggeri, and T P J *Knowles, Science Advance 9*, eabq3151 (2023). DOI: 10.1126/sciadv.abq3151
16. A P Fellows, M T L Casford, and P B Davies, *Biophysical Journal 119*, 1474 (2020). DOI: 10.1016/j.bpj.2020.09.007
17. J Chae, S An, G Ramer, V Stavila, G Holland, Y Yoon, A A Talin, M Allendorf, V A Aksyuk, and A Centrone, *Nano Letters 17*, 5587 (2017). DOI: 10.1021/acs.nanolett.7b02404
18. J Mathurin, A Deniset-Besseau, D Bazin, E Dartois, M Wagner, and A Dazzi, *Journal of Applied Physics 131*, 010901 (2022). DOI: 10.1063/5.0063902
19. S Morsch, S Lyon, S Edmondson, and S Gibbon, *Analytical Chemistry 92*, 8117 (2020). DOI: 10.1021/acs.analchem.9b05793
20. F Tang, P Bao, and Z Su, *Analytical Chemistry 88*, 4926 (2016). DOI: 10.1021/acs.analchem.6b00798
21. M K F Lo, A Dazzi, C A Marcott, E Dillon, Q Hu, K Kjoller, C B Prater, and S W King, *ECS Journal of Solid State Science and Technology 5*, P3018 (2016). DOI: 10.1149/2.0041604jss
22. V W Or, A D Estillore, A V Tivanski, and V H Grassian, *Analyst 143*, 2765 (2018). DOI: 10.1039/C8AN00171E
23. N Qin et al., *Nature Communications 7*, 13079 (2016). DOI: 10.1038/ncomms13079

Bruker Nano Surfaces and Metrology

Santa Barbara, CA • USA
Phone +1.805.967.1400 / 800.873.9750
productinfo@bruker.com

www.bruker.com/nanoIR